Journal of Materials Chemistry A

Accepted Manuscript

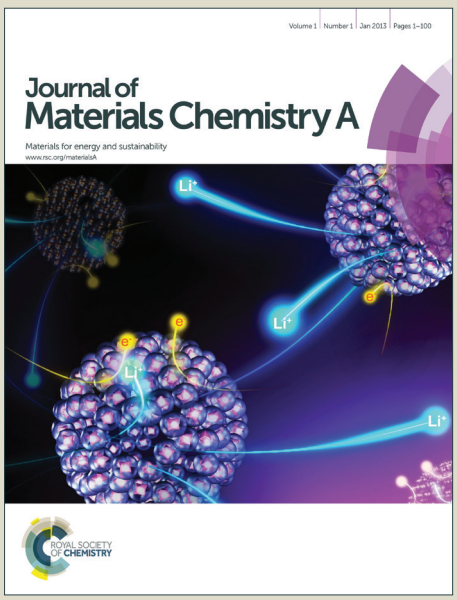

ROYAL SOCIETY OF CHEMISTRY

www.rsc.org/materialsA

Journal Name

RSCPublishing

ARTICLE

A flexible zinc tetrazolate framework with breathing behaviour on xenon adsorption and selective adsorption of xenon over other noble gases

Cite this: DOI: 10.1039/x0xx00000x

Received 00th January 2012,
Accepted 00th January 2012

DOI: 10.1039/x0xx00000x

www.rsc.org/

Shunshun Xiong[a], Qiang Liu[a], Qian Wang[a], Wei Li[a], Yuanming Tang[a], Xiaolin Wang*[a], Sheng Hu*[a] and Banglin Chen[b]

Given the fact that the traditional cryogenic rectification is highly energy and capital intensive during the purification of xenon, effectively selective adsorption of xenon over other noble gases at room temperature using porous materials is a critical and urgent issue. Here we present a flexible zinc tetrazolate framework ($[Zn(mtz)_2]$), which exhibits high capture capacity of xenon and selective adsorption of xenon over other noble gases at room temperature. Due to its high adsorption enthalpy for xenon, the suitable pore size that matches well with xenon atom, as well as the high polarizability of Xe, $[Zn(mtz)_2]$ shows breathing behaviour on xenon adsorption, which is confirmed by experimental adsorption isotherms of xenon and thermodynamic analysis of breathing transition. Isosteric heats of adsorption and S(DIH) calculations indicates that $[Zn(mtz)_2]$ has significantly higher adsorption affinity and capacity for Xe compared with Kr, Ar and N_2. The high capture capacity of Xe (2.7 mmol/g) in idealized PSA process and high Xe/Kr selectivity (15.5) from breakthrough experiment promise its potential application for Xe capture and separation in Xe-Kr gas mixture.

Introduction

The noble gases are important industry commodity and have many significant uses including medical imaging, anesthetics, insulation, commercial lighting and lasers.[1] However, the extremely low concentration of xenon (0.087ppmv) and krypton (1.14 ppmv) in the atmosphere,[2] and the difficulty of its purification, give rise to the high price of noble gases, which imposes restriction on their extensive use. Conventionally, a 20/80 molar mixture of xenon-krypton is obtained as a by-product in cryogenic air separations and must undergo further cryogenic distillation to produce pure xenon and krypton. However, cryogenic process is highly energy and capital intensive. On the other hand, radioisotopes of Xe and Kr, ^{85}Kr and ^{133}Xe for example, are emitted as by-products of nuclear fission and treatment of spent nuclear fuel.[3] Because of the long half-life of ^{85}Kr (10.8 years), separating Kr from Xe to produce pure Xe in Xe-Kr mixture is an important step in removing radioactive ^{85}Kr during treatment of spent nuclear fuel.[3] Hence, capture and selective adsorption of Xe over other noble gases at room temperature is industrially important and remains a critical and urgent issue.

As an alternative to cryogenic processes, separation via selective adsorption at room temperature using porous solids such as zeolites and activated carbons has been investigated.[4] NaA and NaX zeolites can selectively adsorb Xe over Kr with selectivities of approximately four to six, but with low capacities.[5] Tris(o-phenylenedioxy)cyclo-triphosphazene (TPP), a zeolite-like material with a pore diameter of ~4.5 Å can absorb 1.7 $mmolg^{-1}$ Xe at 298K and 1 bar.[6] The emerging Metal-organic frameworks (MOFs), hybrid lattices of organic ligands and metal nodes (metal ions or clusters), have been promised as the cost-effective and efficient materials for gases storage and separation due to their mild synthetic conditions, high thermal stability, high surface areas and controllable pore structures.[7,8] Very recently, effective separation of noble gases using MOFs has received significant attention and become a new focus area.[9-12] Thallapally et al. reported a switch in the Xe-Kr selectivity in FMOFCu at different temperatures.[9a] Li and co-workers showed that $Co_3(HCOO)_6$ can commensurately adsorb Xe and have high IAST selectivity for Xe-Kr.[10] Computational screening studies carried by Snurr et al. suggest that porous materials with cavities diameter of 4.1~8.2 Å would have the highest Xe/Kr selectivity and better materials remain to be discovered.[11] Cooper et al. reported a porous organic cage CC3 with ~4.4 Å cavity showing significantly high selectivity for noble gas separation at low concentrations.[13] Recently, Thallapally et al. reviewed the potential of MOFs for separation of Xe and Kr.[9b] On the other hand, flexible or soft porous networks show reversible structure transitions (breathing or gate-opening) dependent on the nature

and quantity of adsorbed guest molecules and are extremely interesting for applications in selective gas adsorption/separation.[14] However, there is rare systematic investigation of flexible MOFs on selective adsorption of Xe over other noble gases.

In this work, we reported previously a flexible zinc tetrazolate framework, $[Zn(mtz)_2]$ (also named as UTSA-49, UTSA = University of Texas at San Antonio; Hmtz = 5-methyl-1H-tetrazole) exhibits high capture capacity and selective adsorption selectivity for xenon over other noble gases at room temperature. [15] $[Zn(mtz)_2]$ shows a breathing behaviour on Xe adsorption which has been demonstrated by experimental adsorption isotherms of xenon and thermodynamic analysis of breathing transition. The pressure dependent Xe/Kr, Xe/Ar and Xe/N_2 selectivities were calculated using a S(DIH) equation. The Xe capture capacity in an idealized PSA process was calculated to be 2.7 mmol/g. In order to mimic real world conditions, the breakthrough experiment was carried out on a binary gas mixture of xenon-krypton (50/50).

Experimental section

Materials and Measurements:

All reagents and solvents were used as received from commercial suppliers without further purification. Thermogravimetric analyses (TGA) were performed on a Shimadzu TGA-50 analyzer under a nitrogen atmosphere with a heating rate of 3 K min^{-1} from 30 to 800 °C. Powder X-ray diffraction (PXRD) patterns were recorded by a RigakuUltima IV diffractometer operated at 40 kV and 44 mA with a scan rate of 1.0 deg min^{-1}.

Preparation of $[Zn(mtz)_2]$:

A mixture of Hmtz (5.00mg, 0.0079mmol) and $Zn(NO_3)_2 \cdot 6H_2O$ (30.00mg, 0.0587mmol) was dissolved in DMF/EtOH (2.5mL, 4:1, v/v) in a screw-capped vial (20 ml). The vial was capped and placed in an oven at 90℃ for 24 h. The resulting colourless block single crystals were washed with DMF several times to give $[Zn(mtz)_2]$. Elemental analysis: Calcd. for $[Zn(mtz)_2] \cdot (DMF) \cdot H_2O$ ($C_7H_{15}N_9O_2Zn_2$): C, 26.06%; H, 4.69%; N, 39.07%; Found: C, 26.32%; H, 4.77%; N: 38.83%.

Gas Adsorption Measurements:

A QUDRASORB SI-M surface area analyzer was used to measure gas adsorption isotherms. To have a guest-free framework, the fresh sample was guest-exchange with dry methanol 3 times per day for 3 days, filtered and vacuumed at 23 °C for 10 hours to measurements. The activated sample was used for the sorption measurements and was maintained at 77 K with liquid nitrogen and at 273 K with an ice–water bath. As the center-controlled air conditioner was set up at 25 °C, a water bath was used for adsorption isotherms at 298 K. Dry ice/acetonitrile bath was used for isotherm at 220K. For the isotherm at 323K, a temperature-programmed water bath was used. Ultrahigh-purity-grade (>99.999%) N_2, Ar, Xe, Kr and He gases were applied in adsorption measurements.

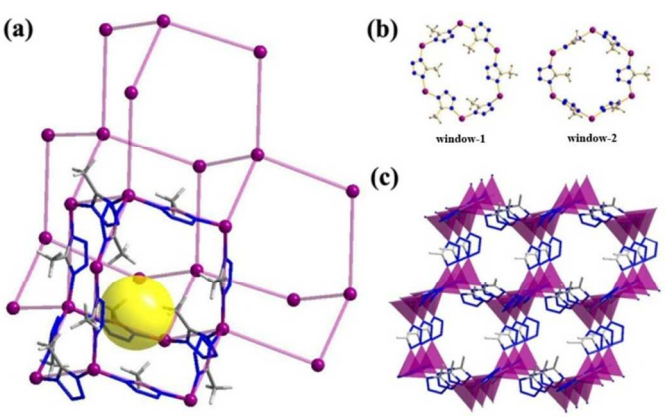

Figure 1. (a) The largest inclusion sphere (yellow sphere) inside the adamantine cage (constructed by 10 Zn^{2+} ions and 12 mtz^- lignds) and the dia topology network of $[Zn(mtz)_2]$ (b) The ball-and-stick model showing the two different 6-membered ring windows: window-1 (left) and window-2 (right) in the adamantine cage of $[Zn(mtz)_2]$ (c) Perspective view of the 3D network of $[Zn(mtz)_2]$. (Zn, purple; C, gray; N, blue; H, white)

Results and discussion

$[Zn(mtz)_2]$ was synthesized according to the procedure (ref 15). The phase purity of the samples was confirmed by Elemental Analysis (EA). As shown in the previous work,[15] $[Zn(mtz)_2]$ has a 3D network with **dia** topology, which is constructed by mtz^- ligands and Zn^{2+} ions. As shown in Figure 1, the adamantine cage in the framework has an internal cavity that is precisely the right size to accommodate a single xenon atom. The diameter of the largest inclusion sphere in this cavity is estimated to be ~4.3Å, which is very close to the diameter of Xe (4.10Å). The adamantine cages pack in the crystalline state to give 3D pore structure and have two kinds of 6-membered Zn-mtz-Zn ring window with the effective aperture size of 2.9 Å × 3.6 Å for window-1 and 3.6 Å × 4.0 Å for window-2, respectively (considering the Van der Waals radii of atoms). The narrowest point, the pore-limiting diameter, for window-1 and window-2 is 2.9Å and 3.6Å, respectively, which is in principle too narrow to permit the diffusion of either Xe or Kr (3.69Å). However, considering the vibrational motion of atoms in the cage molecules in molecular dynamics simulations, window-2 (3.6 Å × 4.0 Å) is broad enough to permit diffusion of Xe and Kr, which has been demonstrated by Cooper's work.[13]

The suitable pore and cavity size for Xe capture encouraged us to examine its potential application on adsorption of Xe. As shown in Figure 2, the Xe low pressure adsorption-desorption isotherms were measured at various temperatures (323K, 298K, 273K and 220K). The Xe uptake of $[Zn(mtz)_2]$ is 3.0 mmol/g (39.2 wt%) at 298K, corresponding to 0.69 Xe molecules per adamantine cage. The Xe uptake at 220K and 1 bar is 4.75 mmol/g and approaches saturation, corresponding to one Xe atom per adamantine cage. Considering its low BET surface area (S_{BET} = 355.3 m^2 g^{-1}), $[Zn(mtz)_2]$ has a high adsorption

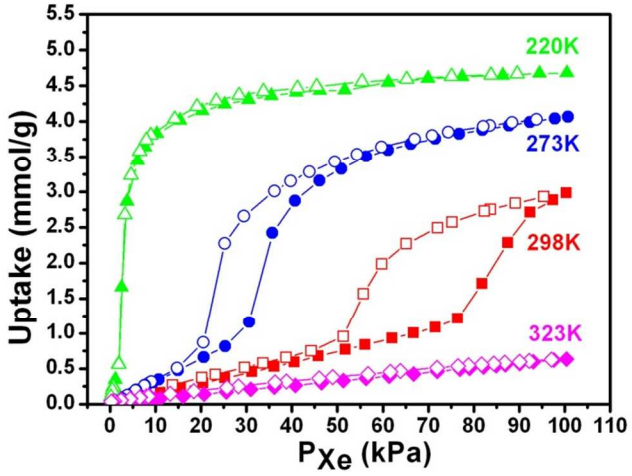

Figure 2. Experimental xenon adsorption isotherms in $[Zn(mtz)_2]$. Filled symbols: adsorption branch; open symbols: desorption branch.

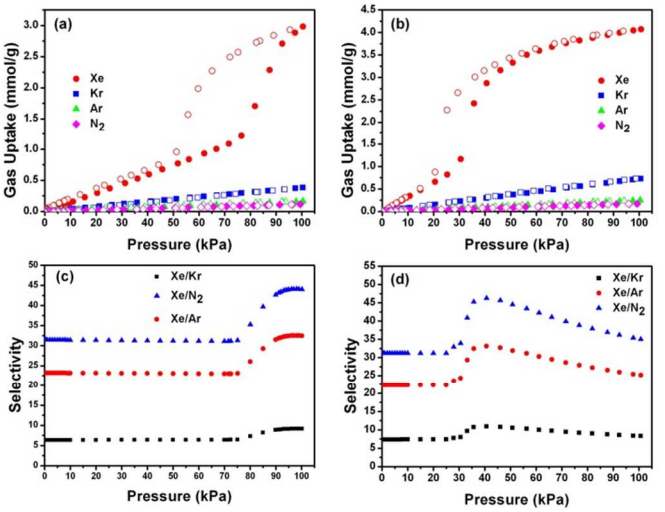

Figure 3. adsorption (solid) and desorption (open) isotherms of xenon (red circles), krypton (blue squares), argon (green triangles) and nitrogen (magenta rhombus) on $[Zn(mtz)_2]$ at 298k (a) and 273 K (b). Pressure-dependent adsorption selectivities of $[Zn(mtz)_2]$ in the equimolar Xe-Kr mixture (black squares), Xe-Ar mixture (red circles) and Xe-N_2 mixture (blue triangles) predicted using a modified DIH equation at 298 (c) and 273 K (d).

capacity of Xe at 298K and 1bar, which is comparable with MIL-53-Al (3.0 mmol/g) and higher than $Co_3(HCOO)_6$ (2.0 mmol/g) and CC3 (~2.3 mmol/g).[10,13,16] The coverage-dependent adsorption enthalpies for Xe were calculated by Clausius-Claperyron equation. The isosteric heat of adsorption ($Q_{st,\ n=0}$) for Xe at zero surface is estimated to be 23.53±0.54 $kJmol^{-1}$. The Q_{st} value for Xe changes dramatically as the amount adsorbed increases and the whole curve looks like a piece of wave, which indicates that the interaction between Xe atoms and pores of the framework transforms during the adsorption of Xe. Although, the Xe enthalpy of $[Zn(mtz)_2]$ is lower than those of HKUST-1 (26.9 kJ mol^{-1}), $Co_3(HCOO)_6$ (29 $kJmol^{-1}$) and CC3 (~25.2 $kJmol^{-1}$), but is still a high value and higher than most reported MOFs, which indicates the strong interaction between the adamantine cage and Xe molecules.[10,12g,13]

It is interesting that $[Zn(mtz)_2]$ exhibits breathing transition during the Xe adsorption and desorption between narrow pore (**np**) and large pore (**lp**) phases. The 273K and 298K isotherms clearly display a phase transition with a hysteresis loop that can be attributed to the **np**-**lp** transition. The 220K isotherm also displays a **np**-**lp** phase transition but without a hysteresis loop. Finally the 323K isotherm shows no sign of phase transition in the accessible pressure range, and the framework is thus believed to remain in the **np** form. Such breathing behaviour on Xe adsorption has been observed on MIL-53.[16] The breathing transition on Xe adsorption is firstly found in such tetrazolate frameworks with a robust **dia** topologic network. It should be noted that only adsorption of Xe can induce structural breathing in $[Zn(mtz)_2]$ and structural breathing doesn't happen during adsorption of other gases (such as Kr, Ar, CO_2, CH_4, N_2) at 298 or 273K. This is different from MIL-53, which exhibits structure transition upon ad sorption of both Xe and CO_2 at room temperature. The special breathing behaviour on Xe adsorption of $[Zn(mtz)_2]$ could be attributed to its right cavity size that matches well with Xe atom, the high adsorption enthalpy for Xe, as well as the higher polarizability of Xe (40.44×10^{-25} cm^3) compared with Kr (24.844×10^{-25} cm^3), Ar (16.411×10^{-25} cm^3) and N_2 (17.403×10^{-25} cm^3).[8f]

Thermodynamic analysis of the data reported in Figure 2 has been carried out using the thermodynamic model developed by Coutert et al.[17] Langmuir fits of the experimental isotherms have been carried as approximations to the "rigid host" isotherms for both **lp** and **np** forms. The ΔF_{host} (free-energy differences) values between **np** and **lp** forms are calculated to be 5.45 and 7.28 kJ mol^{-1} for 298 and 273k, respectively, using the 298 and 273K stepped isotherms (see details in the ESI, Table S4). While, the transition enthalpy value ($\Delta H_{host} = H_{lp}$-H_{np}) and entropy value ($\Delta S_{host} = S_{lp}$-S_{np}) are calculated to be 27 $kJmol^{-1}$ and 73 $JK^{-1}mol^{-1}$, which is comparable with MIL-53 (ΔH_{host} = 15 kJ mol^{-1}, ΔS_{host} = 74 J $K^{-1}mol^{-1}$).

In order to evaluate the potential application of selective adsorption Xe over other gases, the Kr, Ar and N_2 low-pressure adsorption isotherms have also been measured. As shown in Figure 3a, $[Zn(mtz)_2]$ takes up very low amounts of Kr (0.38 mmol/g), Ar (0.16mmol/g) and N_2 (0.11mmol/g) at 298K, compared with Xe. The Q_{st} at zero surface values for Kr, Ar and N_2 were calculated by Clausius-Claperyron equation and estimated to be 16.2, 12.0, and 11.0 $kJmol^{-1}$, respectively. These values are significantly lower than the Q_{st} for Xe, which shows that $[Zn(mtz)_2]$ has much stronger affinity for Xe compared with Kr, Ar and N_2. Different from Xe, the Q_{st} values for all three gases show small variations as a function of uptake, which indicates that $[Zn(mtz)_2]$ exhibits the energetically homogeneous characters of pores during the sorption of Kr, Ar and N_2.

The adsorption selectivities of gases mixtures containing Xe based on the ideal adsorbed solution theory (IAST) is difficult to estimated, since the S shape adsorption isotherm of Xe for $[Zn(mtz)_2]$ can't be fitted well using common Langmuir, dual-site Langmuir, Langmuir-Freundlich and dual-site Langmuir-

Freundlich fitting model. Therefore, we used a S(DIH) equation which has been demonstrated to be precise in prediction of adsorption selectivity for gases mixture in low pressure and requires only the adsorption isotherms and adsorption heats of pure components as input (see details in the ESI).[18] As shown in Figure 3c and 3d, when the pressure is lower than 75 kPa, the adsorption selectivities of Xe/Kr, Xe/Ar and Xe/N_2 (equimolar mixtures) at 298K are 6.4, 23.2 and 31.4, respectively. As the pressure exceeds 75 kPa, the Xe/Kr, Xe/Ar and Xe/N_2 selectivities increase obviously and reach their highest values at 95~100 kPa: 9.2, 32.5 and 44.0 respectively. While, the pressure-dependent adsorption selectivities of Xe/Kr, Xe/Ar and Xe/N_2 at 273K have the same tendency, reach the highest values at 40 kPa: 12.4, 33.1 and 44.6 respectively, but decease gradually after that. This interesting change of adsorption selectivities dependent pressure for [Zn(mtz)$_2$] may be due to the S shape adsorption isotherm (298K and 273K) caused by **np**-**lp** phase transition. Although, the Xe/Kr selectivity at 298K of UTSA- 49 is lower than MOF-74-Co (Henry law selectivity: 10.37 at 298K, 1bar) and $Co_3(HCOO)_6$ (IAST selectivity: 12 at 298K, 1bar), but is still a high value and higher than most reported MOFs.[9,11c,11d] The Xe/N_2 selectivity of [Zn(mtz)$_2$] is also significantly higher than MOF-74-Co (Henry law selectivity: 18.18 at 298K, 1bar), IRMOF-1 (Henry law selectivity: 8.56 at 298K, 1bar) and other reported MOFs.[12c,12d]

Pressure swing adsorption (PSA) or vacuum swing adsorption process (VSA) at moderate temperatures is considered economically feasible in gas separation such as natural or biogas upgrading.[19] In the interest of potentially using [Zn(mtz)$_2$] in swing adsorption processes for Xe capture from Kr in Xe-Kr gas mixture, as would be useful in reprocessing of by-product of air separation. We have estimated the Xe capturing capacity in an idealized PSA process using the Xe adsorption isotherms in Figure 2. The estimates in Figure 4 assume that the gas mixture, by-product after air separation, contains 20 mol% Xe and 80 mol% Kr. The total pressure of the process is assumed to swing from 1 bar to 5 bar in a simple and hypothetical PSA process at 25℃. In the gas mixture, the partial pressure of Xe at 1 bar and 5 bar in the by-product gas corresponds to 0.2 bar and 1 bar, respectively. For these conditions, the Xe capture capacity can be defined as the difference between Xe uptake at 1 bar and 0.2 bar and the represent the moles of Xe gas that can be removed in a PSA cycle per kilogram of the adsorbent. Fig. 4 shows the Xe capture capacity of [Zn(mtz)$_2$] in the highlighted region that corresponds to this PSA condition, i.e. varying pressure from 1 bar to 5 bar. The Xe capture capacity of [Zn(mtz)$_2$] is estimated to be 2.7 and 3.25 mmol/g at 298 and 273K respectively. The Xe capture capacity of [Zn(mtz)$_2$] at 298K is significantly higher than $Co_3(HCOO)_6$ (0.7 mmol/g), CC3 (0.8 mmol/g), MOF-74Ni (2.0 mmolg/g) and similar with Ag@MOF-74Ni (2.7 mmol/g) (see details in the ESI, Fig. S10). Considering the high price of metal Ag on the Ag@MOF-74Ni, [Zn(mtz)$_2$] maybe a more favorable material in reprocessing of by-product of air separation through PSA technology.

To evaluate the feasibility of using [Zn(mtz)$_2$] as a candidate

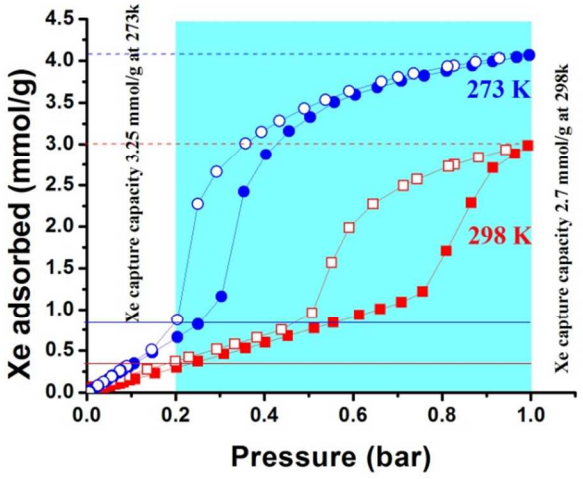

Figure 4. Determination of ideal working capacity of [Zn(mtz)$_2$] in a hypothetical pressure swing adsorption (PSA) cycle. The highlight region represents the working conditions in PSA.

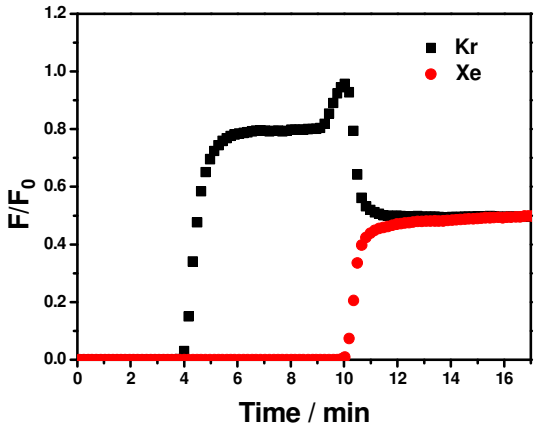

Figure 5. Column breakthrough experiment for a Xe/Kr: 50/50 gas mixture carried out on [Zn(mtz)$_2$] at 296K and 1 bar. (Xe, red circles; Kr, black squares). The flow rate of He and Xe-Kr gas mixture is 10 ml/min.

for separating Kr from Xe in Xe-Kr mixture in real world conditions, we carried out dynamic breakthrough measurements with an adsorption column packed with [Zn(mtz)$_2$] crystals (see details in the ESI). Fig. 5 shows the breakthrough curves for 50:50 mixtures of Xe and Kr on [Zn(mtz)$_2$] at 296K and 1 bar. Kr was detected after the gas mixture was introduced into the column for ~4 minutes. While Xe was not detected until a breakthrough time of 10.5 minutes was reached. It should be noted that the Kr concentration at the column outlet significantly exceeds the feed concentration and has a sharp growth before the Xe is about to pass through the column. This indicates that [Zn(mtz)$_2$] shows significantly stronger interaction for Xe molecules than Kr molecules and the more favoured Xe displaces the already adsorbed Kr during the breakthrough process. The Xe/Kr selectivity was calculated to be 15.5 based on the adsorption capacity of the two gases, which is significantly higher than most reported porous

materials such as Ni/DOBDC, $Co_3(HCOO)_6$, MOF-505 and HUKST-1 and is the highest Xe/Kr selectivity measured by breakthrough experiment using binary Xe-Kr gas mixture.[10,13] These results indicate that $[Zn(mtz)_2]$ exhibits high Xe/Kr selectivity under flow conditions suggesting that it is a promising candidate for Xe capture and separation in Xe-Kr gas mixture.

Conclusions

In summary, we investigated adsorption and separation capacity of a flexible microporous zinc tetrazolate framework, $[Zn(mtz)_2]$, for noble gases in detail. For the first time, we reported a breathing behaviour during the Xe adsorption and desorption on a tetrazolate framework $[Zn(mtz)_2]$ with a rigid **dia** topology, confirmed by experimental adsorption isotherms of xenon and thermodynamic analysis of breathing transition between narrow pore (**np**) and large pore (**lp**) phases. Isosteric heats of adsorption and S(DIH) calculations indicate that $[Zn(mtz)_2]$ has significantly higher adsorption affinity and capacity for Xe compared with Kr, Ar and N_2. The breathing behaviour and preferred adsorption of Xe could be attributed to the high adsorption enthalpy for Xe atoms, the right cavity size that matches well with Xe atom, as well as the high polarizability of Xe. $[Zn(mtz)_2]$ exhibits both high capture capacity of Xe (2.7 mmol/g) in idealized PSA process and high Xe/Kr selectivity (15.5) under flow conditions which promises its potential application for separation of Xe from Kr in Xe-Kr gas mixture.

Acknowledgements

This work was supported by "Radiochemistry 909 Program" in China Academy of Engineering Physics (CAEP), Natural Science Foundation of China (Grants 21402179 and 21301163).

Notes and references

[a] Institute of Nuclear Physics and Chemistry, China Academy of Engineering Physics, Mianyang, Sichuan, 621900, P. R. China. E-mail: xlwang@caep.cn, husheng205@caep.cn.

[b] Department of Chemistry, University of Texas at San Antonio, One UTSA Circle, San Antonio, Texas 78249-069, United States.

† Electronic Supplementary Information (ESI) available: Experimental details, Crystallographic data, PXRD, TGA diagrams, calculation details about the ΔFhost (free-energy differences) value and S(DIH) selectivity are provided. CCDC 988248. For ESI and crystallographic data in CIF or other electronic format see DOI: 10.1039/b000000x/

1 (a) J. Marshall and A. C. Bird, *Br. J. Ophthalmol.*, 1979, **63**, 657-668; (b) G. A. Lane, M. L. Nahrwold, A. R. Tait, M. Taylor-Busch, P. J. Cohen and A. R. Beaudoin, *Science*, 1980, **210**, 899-901; (c) L. T. Liu, Y. Xu, P. Tang, *J. Phys. Chem. B*, 2010, **114**, 9010-9016; (d) P. L. Kebabian, R. R. Romano, A. Freedman, *Meas. Sci. Technol.* 2003, **14**, 983-988; (e) S. Yeralan, D. Doughty, R. Blondia, R. Hamburger, *Proc. SPIEInt. Soc. Opt. Eng.* 2005, **5740**, 27-35. (f) J. D. Stein, P. Challa, *Curr. Opin. Ophthalmol.* 2007, **18**, 140-145.

2 (a) F. G. Kerry, Industrial Gas Handbook: Gas Separation and Purification (CRC Press, 2007).

3 (a) A. Turkevich, L. Winsberg, H. Flotow, and R. M. Adams, *Proc. Natl Acad. Sci.* USA, 1997, **94**, 7807-7810; (b) J. Izumi, In Hand book of Zeolite Science and Technology; S. M. Auerbach, K. A. Carrado, P. K. Dutta, CRC Press: New York, 2003.

4 (a) C. G. Saxton, A. Kruth, M. Castro, P. A. Wright and R. F. Howe, *Microporous Mesoporous Mater.*, 2010, **129**, 68-73; (b) K. A. Carrado, P. K. Dutta and S. M. Auerbach, *Handbook of Zeolite Science and Technology*, Marcel Dekker, New York, 2003; (c) K. Munakata, T. Fukumatsu, S. Yamatsuki, K. Tanaka and M. Nishikawa, *J. Nucl. Sci. Technol.* 1999, **36**, 818–829.

5 (a) C. J. Jameson, A. K. Jameson and H. M. Lim, *J. Chem. Phys.* 1997, **107**, 4364-4372; (b) R. E. Bazan, M. Bastos-Neto, A. Moeller, F. Dreisbach and R. Staudt, *Adsorption*. 2011, **17**, 371-383; (c) K. Munakata, S. Kanjo, S. Yamatsuki, A. Koga and D. Ianovski, *J. Nucl. Sci. Technol.* 2003, **40**, 695-697; (d)

6 G. Couderc, T. Hertzsch, N. R. Behrnd, K. Krämer and J. Hulliger, *Microporous Mesoporous Mater.*, 2006, **88**, 170-175.

7 (a) D. M. D'Alessandro, B. Smit and J. R. Long, *Angew. Chem. Int. Ed.* 2010, **49**, 6058-6082; (b) J. R. Li, Y. G. Ma, M. C. McCarthy, J. Sculley, J. M. Yu, H. K. Jeong, P. B. Balbuena and H. C. Zhou, *Coord. Chem. Rev.*, 2011, **255**, 1791-1823; (c) K. Sumida, D. L. Rogow, J. A. Mason, T. M. McDonald, E. D. Bloch, Z. R. Herm, T.-H. Bae and J. R. Long, *Chem. Rev.*, 2012, **112**, 724-781; (d) T. C. Drage, C. E. Snape, L. A. Stevens, J. Wood, J. Wang, A. I. Cooper, R. Dawson, X. Guo, C. Satterley and R. Irons, *J. Mater. Chem.* 2012, **22**, 2815-2823; (e) J. Liu, P. K. Thallapally, B. P. McGrail, D. R. Brown and J. Liu, *Chem. Soc. Rev.*, 2012, **41**, 2308–2322; (f) Z. Zhang, Z.-Z. Yao, S. Xiang and B. Chen, *Energy Environ. Sci.*, 2014, **7**, 2868-2899.

8 (a) O. Shekhah, Y. Belmabkhout, Z. Chen, V. Guilerm, A. Cairns, K. Adil and M. Eddaoudi, *Nat. Commun.* 2014, **5**, 4228; (b) P. Nugent, Y. Belmabkhout, S. D. Burd, A. J. Cairns, R. Luebke, K. Forrest, T. Pham, S. Ma, B. Space, L. Wojtas, M. Eddaoudi and M. J. Zaworotko, *Nature*, 2013, **495**, 80-84; (c) B. Li, H.-M. Wen, W. Zhou and B. Chen, *J. Phys. Chem. Lett.*, 2014, **5**, 3468; (d) Y. He, W. Zhou, R. Krishnaand B. Chen, *Chem. Coummun.* 2012, **48**, 10856; (e) S. Xiang, Y. He, Z. Zhang, H. Wu, W. Zhou, R. Krishna and B. Chen, *Nat. Commun.* 2012, **3**, 954; (f) J-R. Li, R. J. Kuppler and H-C. Zhou, *Chem. Soc. Rev.*, 2009, **38**, 1477-1504.

9 (a) C. A. Fernandez, J. Liu, P. K. Thallapally and D. M. Strachan, *J. Am. Chem. Soc.*, 2012, **134**, 9046–9049; (b) D. Banerjee, A. J. Cairns, J. Liu, R. K. Motkuri,S. K. Nube, C. A. Fernandez, R. Krishna, D. M. Strachan and P. K. Thallapally, *Acc. Chem. Res.* 2014, DOI: 10.1021/ar5003126.

10 H. Wang, K. Yao, Z. Zhang, J. Jagiello, Q. Gong, Y. Han and J. Li. *Chem. Sci.*, 2014, **5**, 620-624.

11 B. J. Sikora, C. E. Wilmer, M. L. Greenfield and R. Q. Snurr, *Chem. Sci.* 2012, **3**, 2217-2223.

12 (a) P. K. Thallapally, J. W. Grate and R. K. Motkuri. *Chem. Commun.*, 2012, **48**, 347-349; (b) J. Liu, P. K. Thallapally and D. Strachan. *Langmuir*. 2012, **28**, 11584-11589; (c) S. T. Meek, S. L. Teich-McGoldrick, J. J. Perry IV, J. A. Greathouse and M. D. Allendorf. *J. Phys. Chem. C.* 2012, **116**, 19765-19772; (d) J. J. Perry-IV, S. L. Teich-McGoldrick, S. T. Meek, J. A. Greathouse, M. Haranczyk and M. D. Allendorf. *J. Phys. Chem. C.* 2014, **118**, 11685-11698; (e) J. Liu, D. M. Strachan and P. K. Thallapally.

Chem. Commun., 2014, **50**, 466-468; (f) Y.-S. Bae, B. G. Hauser, Y. J. Colon, J. T. Hupp, O. K. Farha and R. Q. Snurr, *Microporous Mesoporous Mater.*, 2013, **169**,176-179; (g) A. S. Dorcheh, D. Denysenko, D. Volkmer, W. Donner and M. Hirscher, *Microporous Mesoporous Mater.*, 2012, **162**, 64–68; (h) Q. Wang, H. Wang, S. M. Peng, X. Peng and D. P. Cao, *J. Phys. Chem. C.*, 2014, **118**, 10221-10229; (i) J. Liu, C. A. Fernandez, P. F. Martin, P. K. Thallaplly, and D. M. Strachan, *Ind. Eng. Chem. Res.*, 2014, **32**, 12893-12899.

13 L. Chen, P. S. Reiss, S. Y. Chong, D. Holden, K. E. Jelfs, T. Hasell, M. A. Little, A. Kewley, M. E. Briggs, A. Stephenson, K. M. Thomas, J. A. Armstrong, J. Bell, J. Busto, R. Boel, J. Liu, D. M. Strachan, P. K. Thallapally and A. I. Cooper. *Nat. Mater.* 2014, **134**, 18892-18895.

14 (a) L. Alaerts, C. E. A. Krschhock, M. Maes, M. A. van der Veen, V. Finsy, A. Depla, J. A. Martens, G. V. Baron, P. A. Jacobs, J. E. M. Denayer and D. E. De Vos, *Angew. Chem., Int. Ed.*, 2007, **46**, 4293; (b) R. Kitaura, K. Seki, G. Akiyama and S. Kitagawa, *Angew. Chem., Int. Ed.*, 2003, **42**, 428; (c) M. Kondo, T. Okbo, A. Asami, S.-I. Noro, T. Yoshitomi, S. Kitagawa, T. Ishii, H. Matsuzaka and K. Seki, *Angew. Chem., Int. Ed.*, 1999, **38**, 140; (d) N. Klein, C. Herzog, M. Sabo, I. Senkovska, J. Getzscmann, S. Paasch, M. R. Lohe, E. Brunner and S. Kaskel. *Phys. Chem. Chem. Phys.*, 2010, **12**, 11778-11784; (e) S. Henke, R. Schmid, J.-D. Grunwaldt and R. A. Fisher. *Chem. Eur. J.* 2010, **16**, 14296-1430; (f) J.-R. Li, J. Sculley and H.-C. Zhou, *Chem. Rev.* 2012, **112**, 869–932; (g) G. Férey and C. Serre. *Chem. Soc. Rev.*, 2009, **38**, 1380-1399.

15 S. Xiong, Y. Gong, H. Wang, H. Wang, Q. Liu, M. Gu, X. Wang, B. Chen and Z. Wang. *Chem. Commun.*, 2014, **50**, 12101-12014.

16 A. Boutin, M.-A. Springuel-Huet, A. Nossov, A. Gédéon, T. Loiseau, C. Volkringer, G. Férey, F.-X. Coudert and A. H. Fuchs. *Angew. Chem. Int. Ed.* 2009, **48**, 8314-8317.

17 F.-X. Coudert, M. Jeffroy, A. H. Fuchs, A. Boutin and C. Mellot-Draznieks. *J. Am. Chem. Soc.* 2008, **130**, 14294-14302.

18 H. Wang, X. Zeng and D. Cao. *J. Mater. Chem. A.* 2014, **2**, 11341-11348.

19 (a) R. P. Lively, R. R. Chance and W. J. Koros, *Ind. Eng. Chem. Res.*, 2010, **49**, 7550–7562; (b) J. M. Simmons, H. Wu, W. Zhou and T. Yildirim, *Energy Environ. Sci.*, 2011, **4**, 2177–2185; (c) L. Bastin, P. S. Barcia, E. J. Hurtado, J. A. C. Silva,A. E. Rodrigues and B. Chen, *J. Phys. Chem. C*, 2008, **112**, 1575–1581.

TOC

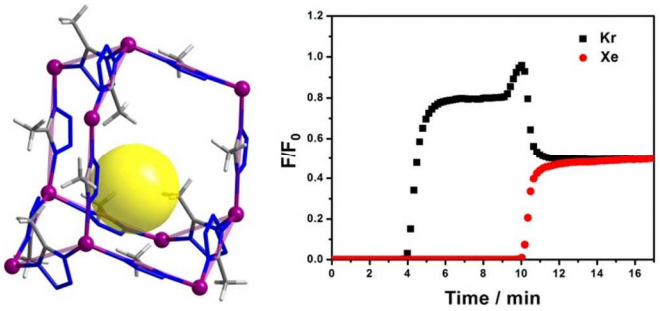

A flexible zinc tetrazolate framework shows breathing behaviour on xenon adsorption, due to its high adsorption enthalpy for xenon, the suitable pore size that matches well with xenon atom and the high polarizability of Xe. The high capture capacity of xenon, as well as high Xe/Kr, Xe/Ar and Xe/N_2 separation selectivities promise its potential application for selective adsorption of Xe over other noble gases.